Loss of histone H4 lysine 20 trimethylation in osteosarcoma is associated with aberrant expression ofhistone methyltransferase SUV420H2

LIANHUA PIAO[1*], XIAOFENG YUAN[2*], LUHUI WANG[2], XIAOSHUANG XU[1], MING ZHUANG[2], JINGGAO LI[3], REN KONG[1] and ZHIWEI LIU[2]

[1]Institute of Bioinformatics and Medical Engineering, Jiangsu University of Technology, Changzhou, Jiangsu 213001; [2]Department of Orthopaedics, The Third Affiliated Hospital of SooChow University, Changzhou, Jiangsu 213000; [3]School of Computer Engineering, Jiangsu University of Technology, Changzhou, Jiangsu 213001, P.R. China

Received March 23, 2020; Accepted June 17, 2020

DOI: 10.3892/ol.2020.11887

Abstract. Epigenetic modifications of histones have crucial roles in various types of cancers. The aberrant trimethylation of histone H4 at lysine 20 (H4K20) has been implicated in carcinogenesis. At present, the status of trimethylation at H4k20 (H4K20me3) in osteosarcoma (OS), the predominant bone cancer in humans, is unknown. In the present study, a genome-wide decrease was observed in H4K20me3 levels in OS tissues and cell lines. Reduced levels of lysine methyltransferase 5C (SUV420H2), the histone methyltranferase responsible for modification of H4K20me3, was also observed in OS cells with the associated loss of H4K20me3. Furthermore, a total of 507 SUV420H2-regulated genes were identified through RNA-seq and a number of candidate genes were further validated. Bioinformatic analysis revealed an association between SUV420H2 and multiple signaling pathway, including the mitogen-activated protein kinase, P53, transforming growth factor and the ErbB pathways. These results demonstrated that there are aberrant levels of H4K20me3 and SUV420H2 in OS, and highlighted H4K20me3 as a candidate biomarker for the early detection of OS.

Introduction

Osteosarcoma (OS) is the most common primary malignancy of bone, which also has a high rate of metastasis to the lungs (1). Currently, the 5-year survival for patients with localized OS is 60-65%; however, survival drops to 20-30% for patients with recurrent disease (2). Despite various attempts, the overall survival probabilities have not substantially improved in the last 30 years (2). OS is a heterogeneous tumor, with a wide diversity of genetic and epigenetic alterations that are involved in its development and progression (1,3). As such, the identification of these genetic and epigenetic abnormalities may have a great impact on the future therapies for OS.

Epigenetic regulations through post-translational modifications (PTMs) of histone proteins by methylation have been characterized as key factors in cell growth, differentiation and DNA repair pathways (4,5). Aberrant histone methylation is a universal feature of various types of cancer and most likely plays a causal part in tumorigenesis (6,7). However, due to the rarity of OS within the population, there are limited studies investigating alterations of histone methylation in OS. To the best of our knowledge, the present study is the first showing aberrant histone methylation in OS.

Methylation of histone H4 lysine20 (H4K20) is implicated genomic integrity, such as playing a role in the DNA repair, DNA replication, chromatin compaction and transcriptional regulation processes (8,9). Trimethylation at H4K20 (H4K20me3), a marker of constitutive heterochromatin, is correlated with the silencing of genes during the development of various types of cancer (10,11). In particular, a global decrease of H4K20me3 is considered a common hallmark of various types of human cancers (11-14). It has been proposed that the loss of H4K20me3 in repetitive DNA sequences is associated with the global loss of DNA methylation in tumorigenesis (11). Furthermore, loss of H4K20me3 is correlated with a poor prognosis in bladder, colon and breast cancer, presenting H4K20me3 with a potential prognostic value for various types of cancer (15-20). Lysine methyltransferase 5B (SUV420H1) and lysine methyltransferase 5C (SUV420H2) are preferentially responsible for dimethylation of H4K20 (H4K20me2) and trimethylation of H4K20 (H4K20me3)(21,22).Suv420h-double-null(Suv420h1/Suv420h2 double-knockout) mice present with perinatally death and lose nearly all H4K20me2 and H4K20me3, as well as being accompanied with chromosomal aberrations and deficiencies in DNA double-strand break repair (23). Abrogation of SUV420H2 or

Correspondence to: Dr Zhiwei Liu, Department of Orthopaedics, The Third Affiliated Hospital of SooChow University, 185 Juqian Street, Changzhou, Jiangsu 213000, P.R. China
E-mail: liuzhiweil@126.com

*Contributed equally

Key words: lysine methyltransferase 5C, histone H4 lysine 20, osteosarcoma, histone methyltransferase, epigenetics

both SUV420H HMTs but not SUV420H1 leads to decreased H4K20me3 in telomeric chromatin that provides an increased tumorigenic potential, indicating an important role for SUV420H HMTs in tumorgenicity (24,25). In the present study, aberrations in histone H4K20 trimethylation in OS tissues and cell lines were observed, presumably associated with decreased SUV420H2 expression levels, which is likely to be related to a poor survival in OS. Additionally, a set of SUV420H2-regulated genes involved in numerous signaling pathways was identified through RNA-sequencing (RNA-seq) analysis. As such, the present findings indicated crucial functions for H4K20me3 and its specific HMTs, SUV420H2, in OS. Furthermore, it was illustrated that H4K20me3 and SUV420H2 may be promising candidate biomarkers for the early detection of OS.

Materials and methods

Cell lines and cell culture. The human osteoblast cell line, hFOB1.19, and human OS cell lines, HOS, U2OS and MG-63, were purchased from The Cell Bank of Type Culture Collection of the Chinese Academy of Sciences. Cells were grown in DMEM (Gibco; Thermo Fisher Scientific, Inc.), supplemented with 10% FBS (ScienCell Research Laboratories, Inc.) and 1% antibiotic/antimycotic solution (Gibco; Thermo Fisher Scientific, Inc.) at 37˚C in a humidified incubator with 5% CO_2.

RNA extraction and reverse transcription-quantitative PCR (RT-qPCR). Total RNA was isolated from the cells by using Takara MiniBEST Universal RNA Extraction kit (Takara Bio, Inc.). RNA was reverse transcribed to cDNA using the PrimeScript™ 1st strand cDNA Synthesis kit (Takara Bio, Inc.) according to the manufacturer's instruction. The cDNA synthesis reaction was performed at 42˚C for 45 min. Quantitative PCR was conducted using TB Green™ Premix Ex Taq™ II (Takara Bio, Inc.) at 95˚C for 30 sec, followed by 40 cycles of 95˚C for 5 sec and 60˚C for 34 sec, in the ABI StepOnePlus Real-time PCR system (Applied Biosystems; Thermo Fisher Scientific, Inc.). Relative gene expression levels were quantified relative to GAPDH levels using the $2^{-\Delta\Delta Cq}$ method (26). Each sample was analyzed in triplicate. The primer sequences are listed in Table SI.

Small interfering RNA (siRNA) transfection. siRNA oligonucleotide duplexes were synthesized by Biolino Nucleic Acid Technology Co., Ltd. (www.biolino.cn), targeting the human *SUV420H2* transcripts. siRNA targeting enhanced green fluorescent protein [EGFP (siEGFP)] and negative control (siNC) were used as control siRNAs. The siRNA sequences are described in Table SII. OS cancer cells were transfected with siRNA duplexes (100 nM final concentration) using Lipofectamine® RNAiMAX (Thermo Fisher Scientific, Inc.). Lipofectamine® RNAiMAX and siRNA were separately diluted in Opti-MEM® I Reduced Serum Medium (Gibco; Thermo Fisher Scientific, Inc.). Two diluted reactions were mixed together, incubated for 5 min at room temperature, and the siRNA-lipid complex was added to cells. Transfected cells were incubated continuously at 37˚C for additional 96 h followed by immediate RNA extraction or cell lysis.

Immunohistochemistry (IHC), western blotting (WB) and antibodies. Pre-fixed human OS tissue microarray containing 43 OS samples and 13 normal bone samples (from adjacent normal bone tissue) was purchased from Alenabio. EliVision™ plus kit and DAB kit (MXB Biotechnologies; http://maxim.com.cn/) were used for staining according to the manufacturer's instruction. The sections were deparaffinized with xylene and rehydrated through 100, 95, 85 and 70% ethanol for 5 min. Endogenous peroxidase activity was blocked by incubating sections in 3% H_2O_2 solution in methanol at room temperature for 10 min. After blocking with 10% goat serum (Wuhan Boster Biological Technology, Ltd.) at room temperature for 20 min, the sections were sequentially incubated with rabbit anti-H4K20me3 antibody (1:100) at 37˚C for 2 h, signal enhancer (from the EliVision™ Plus kit, MXB Biotechnologies) at room temperature for 30 min and anti-rabbit IgG Fab-HRP (ready to use, EliVision™ Plus kit) at 37˚C for 30 min. Each incubation step was followed by three washes in PBS for 5 min. DAB solution (DAB kit, MXB Biotechnologies) was applied to reveal the color. After the color development was stopped by washing with distilled water, the slides were immersed into hematoxylin at room temperature for 10 min and washed with distilled water. The slides were dehydrated through 4 changes of ethanol (70, 85, 95 and 100%) for 5 min each, cleared with xylene, and mounted using Neutral balsam mounting solution (Sinopharm Chemical Reagent Co., Ltd.). Finally, the tissue slides were observed under a light microscope at 200x and 400x magnification (Olympus BX41). Two expert pathologists performed semiquantitative analysis of H4K20me3 staining levels using a 3-grade scale defined as: Mild grade, +1; moderate grade, +2; and strong grade, +3. For WB, the cells were lysed using RIPA lysis buffer [50 mM Tris-HCl (pH 7.4), 150 mM NaCl, 0.5% sodium deoxycholate, 0.1% SDS, 1% Nonidet-P40, 0.1 mM PMSF] containing Protease Inhibitor Cocktail (Roche Diagnostics), and protein concentrations were determined using a BCA Protein assay kit (CoWin Biosciences). In total, 20 μg proteins were loaded in each well then subjected to 10% (for detection of SUV420H2 and β-actin) or 15% (for detection of H4K20me3 and H4) SDS-PAGE. The proteins were transferred onto polyvinylidene fluoride (PVDF) membranes followed by blocking with 5% milk in 0.1% TBST buffer for 1 h at room temperature. Later, the blots were incubated with primary antibodies at 4˚C overnight, and subsequently incubated with secondary antibodies for 1 h at room temperature. Finally, the protein signals were detected by Tanon high-sig ECL western blotting substrate (Tanon Science & Technology Co., Ltd.). The relative density of the protein band of interest is qualified using Tanon Image Software version 1.0 (Tanon Science & Technology Co., Ltd.). The following antibodies were used: Anti-H4K20me3 (cat. no. ab9053; dilution, 1:100 for IHC and 1:1,000 for WB; Abcam), anti-H4 (cat. no. 16047-1-AP; dilution, 1:500; ProteinTech Group, Inc.), anti-SUV420H2 antibody (cat. no. ab91224; dilution: 1:100; Abcam), anti-β-actin (cat. no. sc-47778; dilution, 1:1,000; Santa Cruz Biotechnology, Inc.), goat anti-rabbit IgG secondary antibody, HRP conjugate (cat. no. KGAA35; dilution: 1:1,000; KeyGEN BioTECH) and goat anti-mouse IgG secondary antibody, HRP conjugate (cat. no. KGAA37; dilution, 1:1,000; KeyGEN BioTECH).

RNA-seq analysis. Indexed libraries from HOS cells incubated with siEGFP or siSUV420H2 were subjected to RNA-seq using the Illumina Hiseq2000 platform (Illumina, Inc.). Gene

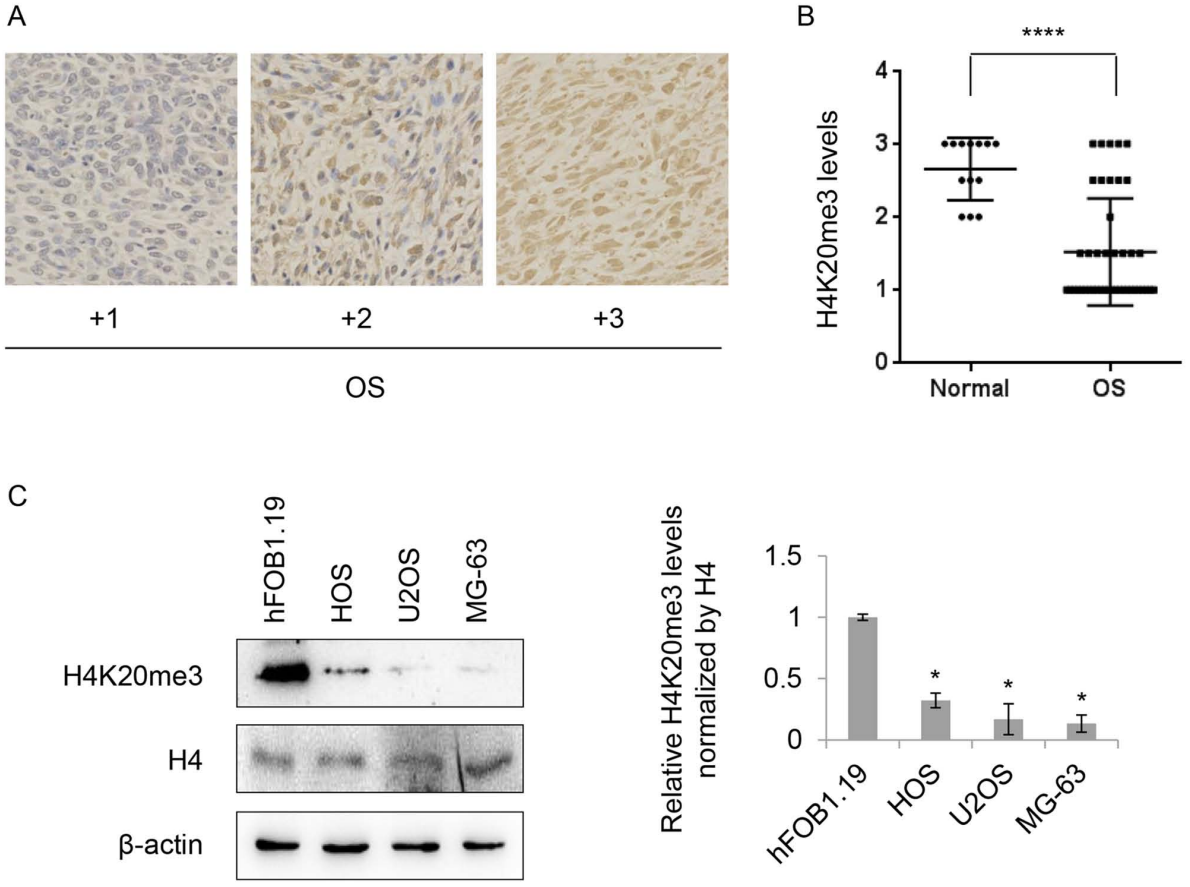

Figure 1. Modifications to H4K20me3 in OS. (A) Representative samples of H4K20me3 immunostaining in tissue samples (400x magnification) from patients with OS, ranging from low (+1) to high (+3). H4K20me3 positive spots exhibited brown staining with a nuclear localization. (B) Levels of H4K20me3 were significantly lower in the OS samples than in normal bone tissue. (C) H4K20me3 levels were reduced in HOS, U2OS and MG-63 osteosarcoma cell lines compared to hFOB1.19 cells. Histone H4 and β-actin served as loading controls. Data are presented as the mean ± standard deviation of two independent experiments; *P<0.05 OS cell lines vs. hFOB1.19. ****P<0.0001. H4, histone H4; H4k20me3, trimethylation at histone H4 lysine 20; OS, osteosarcoma.

expression was quantified using the fragments per kilobase of transcript per million mapped reads (FPKM) normalization method (27) and Cufflinks version 2.2.1 (http://cole-trapnell-lab.github.io/cufflinks/install/) was used for FPKM quantification. Gene expression levels and differential transcription between siEGFP and siSUV420H2 treated cells (using the same methodology as aforementioned) were evaluated using Cuffdiff (part of the Cufflinks software aforementioned). The lists of significantly differentially expressed genes were obtained using a threshold of P-value ≤0.05 and a fold-change ≥2. Gene Ontology (GO) analysis was performed using the standard enrichment computation method (28). KEGG pathway analysis was performed by KOBAS and P<0.05 was set as the cut-off criterion.

Statistical analysis. Statistical analyses were performed using SPSS version 20.0 (IBM Corp.). Comparisons between two groups were analyzed using an independent two-sample t-test (two-tailed), while comparisons among multiple groups were analyzed using one-way ANOVAs followed by Tukey's post hoc test. P<0.05 was considered to indicate a statistically significant difference. Experiments were performed in duplicate or triplicates and results are presented as mean ± SD except for the RT-qPCR experiments. The mean ± SEM was used for RT-qPCR experiments. The status of overall survival regarding the SUV420H2 expression was set using the median SUV420H2 expression as the cut-off and was estimated with the Kaplan-Meier method using GraphPad Prism v.6 software (GraphPad Software, Inc.). The log-rank test was used to assess statistical significance.

Results

Aberrant pattern of H4K20me3 in OS. The expression status of H4K20me3 was examined in tissue samples from patients with OS using a tissue microarray containing 43 OS samples and 13 normal bone samples (from adjacent normal bone tissue) by IHC analysis. Fig. 1A presents representative results of the IHC data, where scores were applied of +1 to +3. IHC analysis revealed moderate or strong (≥+2) staining of H4K20me3 in all of normal samples (13 in 13) compared with 25.58% (11 in 43) in the OS cases. Approximately 55.81% (24 in 43) of OS cases expressed H4K20me3 at mild levels (+1) and 18.6% (8 in 43) of OS cases between mild to moderate levels (Fig. 1B), indicating decreased levels of H4K20me3 in OS tissues. Subsequently, the levels of H4K20me3 in OS cell lines were investigated. The levels of H4K20me3 were reduced in all of three tested OS cell lines (HOS, U2OS and MG-63) compared with the normal osteoblast cell line, hFOB1.19, whereas there was no significant change in the expression of total histone H4 (Fig. 1C). Together, these results illustrated that there was a loss of H4K20me3 in both the OS tissues and cancer cell lines.

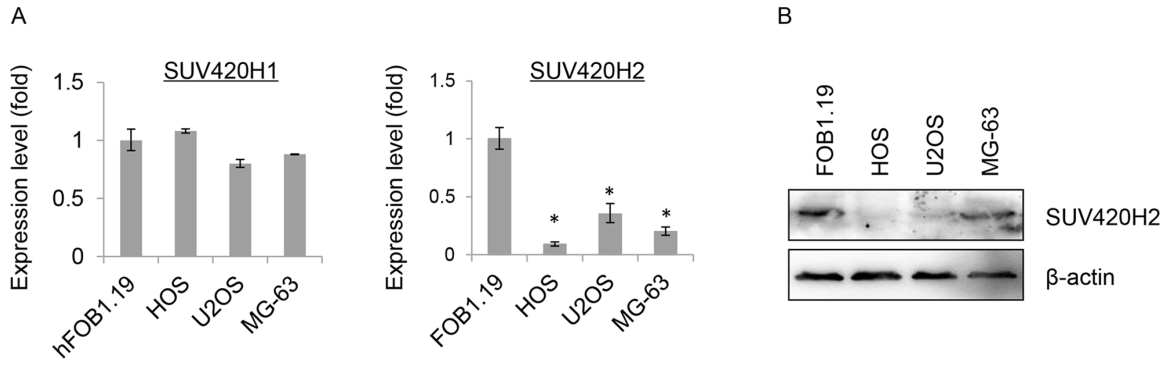

Figure 2. Reduced expression levels of SUV420H2 are found in OS cell lines. (A) Reverse transcription-quantitative PCR of SUV420H1 (left) and SUV420H2 (right) in OS cell lines, compared with the normal control hFOB1.19 cell line. mRNA expression levels were normalized to GAPDH. Data are presented as the mean ± SEM of three independent experiments; *P<0.05 OS cell lines vs. hFOB1.19. (B) Expression of SUV420H2 protein in OS cell lines was analyzed by WB analysis using anti-SUV420H2 antibodies and β-actin served as a loading control. OS, osteosarcoma; SUV420H1, lysine methyltransferase 5B; SUV420H2, lysine methyltransferase 5C.

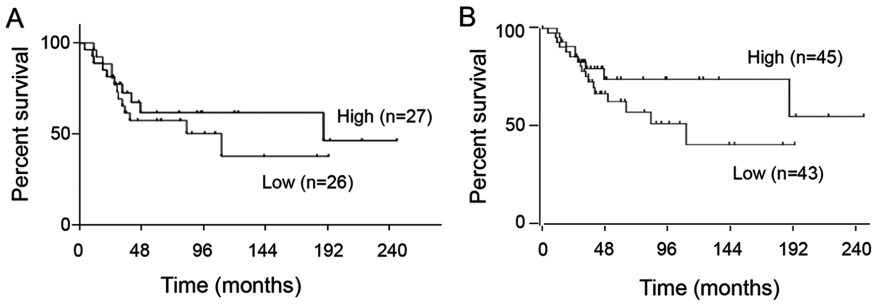

Figure 3. Kaplan-Meier overall survival for patients with osteosarcoma in the (A) GSE21257 and (B) GSE42352 database based on SUV420H2 expression levels (low vs high expression level groups). SUV420H2, lysine methyltransferase 5C.

SUV420H2 expression is associated with decreased H4K20me3 levels in OS. To identify the histone methyltransferase responsible for the loss of H4K20me3, the mRNA expression levels of both SUV420H1 and SUV420H2 were examined. Interestingly, only mRNA expression levels of SUV420H2 were significantly reduced in all three OS cell lines (HOS, U2OS and MG-63) compared to hFOB1.19 cells, but not mRNA expression levels of SUV420H1 (Fig. 2A). Similarly, a drastic reduction in protein expression levels of SUV420H2 were observed in HOS, U2OS and MG-63 cells in contrast to hFOB1.19 cells, indicating that the decreased SUV420H2 is associated with the global loss of H4K20me3 in OS (Fig. 2B). The present study failed to detect the protein expression of SUV420H1 in cell lines due to the antibody issue. Next, using the expression profile dataset GSE21257, which included 53 OS samples, and the GSE42352 dataset, which included 88 OS samples, the prognostic significance of SUV420H2 expression was investigated. As shown in Fig. 3A and B, no prognostic value for SUV420H2 expression was observed (P=0.47 in GSE21257; P=0.11 in GSE42352). Nevertheless, there was a tendency towards a poorer prognosis in low SUV420H2 expression group even though the association was not significant.

Identification of downstream genes of SUV420H2. To identify the involvement of SUV420H2 in OS, RNA-seq analysis was performed to find SUV420H2-regulated genes in HOS cells which were expressed at higher levels with H4K20me3. The knockdown efficiency of SUV420H2 was validated both at the mRNA and protein levels, as shown in Fig. 4A and B. The expression levels of SUV420H2 were substantially reduced in the siSUV420H2 treated cells. Subsequently, RNA sequencing of the gene expression analysis was performed in HOS cells treated with siSUV420H2#1 or siEGFP as a control. A variety of genes were identified, including 205 upregulated genes and 302 downregulated genes in SUV420H2-depleted HOS cells, with a threshold of P≤0.05 and a fold-change ≥2 as compared with the control (Fig. 4C). GO term enrichment analysis of the biological process category revealed that upregulated genes after SUV420H2 depletion were involved in various biological processes, including regulation of cell proliferation (GO:0042127, 35 upregulated DEGs were included), regulation of growth (GO:0040008, 20 upregulated DEGs were included) and the response to chemicals (GO:0042221, 40 upregulated DEGs were included), whereas downregulated genes after SUV420H2 depletion were associated with the negative regulation of transcription (GO:0045892, 42 downregulated DEGs were included), regulation of metabolic processes (GO:0019222, 127 downregulated DEGs were included) and the negative regulation of gene expression (GO:0010629, 41 downregulated DEGs were included) (Fig. 5A), indicating that SUV420H2 expression is involved with a complicated of functions *in vivo*. Additionally, the top ten KEGG pathways were analyzed and presented in Fig. 5B.

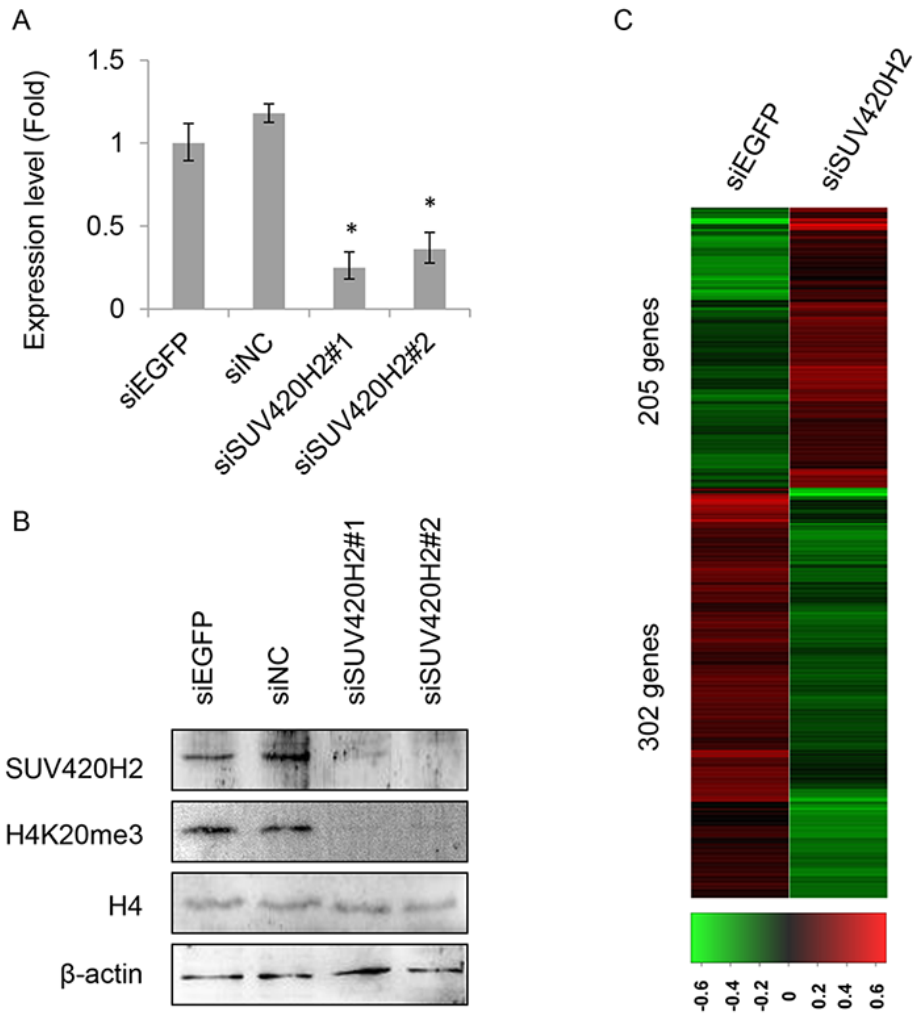

Figure 4. Downstream genes of SUV420H2 were identified using RNA-sequencing. (A) Reverse transcription-quantitative PCR was used to examine the knockdown effect of SUV420H2 expression in HOS cells transfected with siRNA specific to SUV420H2 (si SUV420H2#1 and si SUV420H2#2) compared to control siRNA (siEGFP and siNC). Data are presented as the mean ± SEM of three independent experiments. (B) The knockdown efficiency of SUV420H2 in protein level was confirmed using western blotting. Levels of H4K20me3 were also investigated. Total histone H4 and β-actin were loaded as controls. (C) Heatmap of up and downregulated genes following depletion of SUV420H2. RNA sequence analyses were conducted on HOS cells treated with SUV420H2-specific siRNA (si SUV420H2#1) or EGFP control siRNA for 96 h. *P<0.05 vs. siEGFP. EGFP, enhanced green fluorescent protein; H4K20me3, trimethylation at histone H4 lysine20; si, small interfering RNA; SUV420H2, lysine methyltransferase 5C.

These results demonstrated that changes in SUV420H2 expression may influence a variety of key signaling pathways in carcinogenesis including the mitogen-activated protein kinase (MAPK), p53 and ErbB signaling pathways, indicating substantial contributions of SUV420H2 to carcinogenesis. To validate the findings of the RNA-seq, the top 20 upregulated and downregulated candidate genes were selected for further analysis using RT-qPCR. Two SUV420H2 specific siRNAs (siSUV420H2#1 and siSUV420H2#2), targeting different sections of SUV420H2, were used to exclude any off-target candidate genes. As a result, 7 upregulated and 13 downregulated genes, as listed in Fig. 6A and B, were identified from the depletion of SUV420H2. Fos proto-oncogene (FOS), which is implicated as a regulator of cell proliferation and differentiation (29) and was upregulated with the reduction in SUV420H2 expression. Growth differentiation factor 15, which is involved in transforming growth factor (TGF) signaling (30), was downregulated with the silencing of SUV420H2.

Discussion

The nucleosome is comprised of histone proteins containing a 147-bp DNA segment and is a fundamental unit of chromatin structures (31). All four core histone proteins, including H3, H4, H2A and H2B undergo diverse PTMs such as acetylation, phosphorylation, methylation, ubiquitination, SUMOylation and ADP-ribosylation (32). Through dynamic regulations of chromatin structure, these histone modifications impact on genomic integrity and a set of physiological functions, including transcriptional regulation and DNA replication, as well as DNA damage and repair (4,5). Among these histone modifications, aberrant histone methylation events are likely to play a causal role in tumorigenesis (6). H4K20me3, a hallmark of silenced heterochromatic regions, is closely related with various types of cancer (10). Aberrant H4K20me3 has been reported in breast and lung cancers (11,13,14). However, there is no reported study regarding the status of H4K20me3 in OS. As such, the present study firstly examined the levels

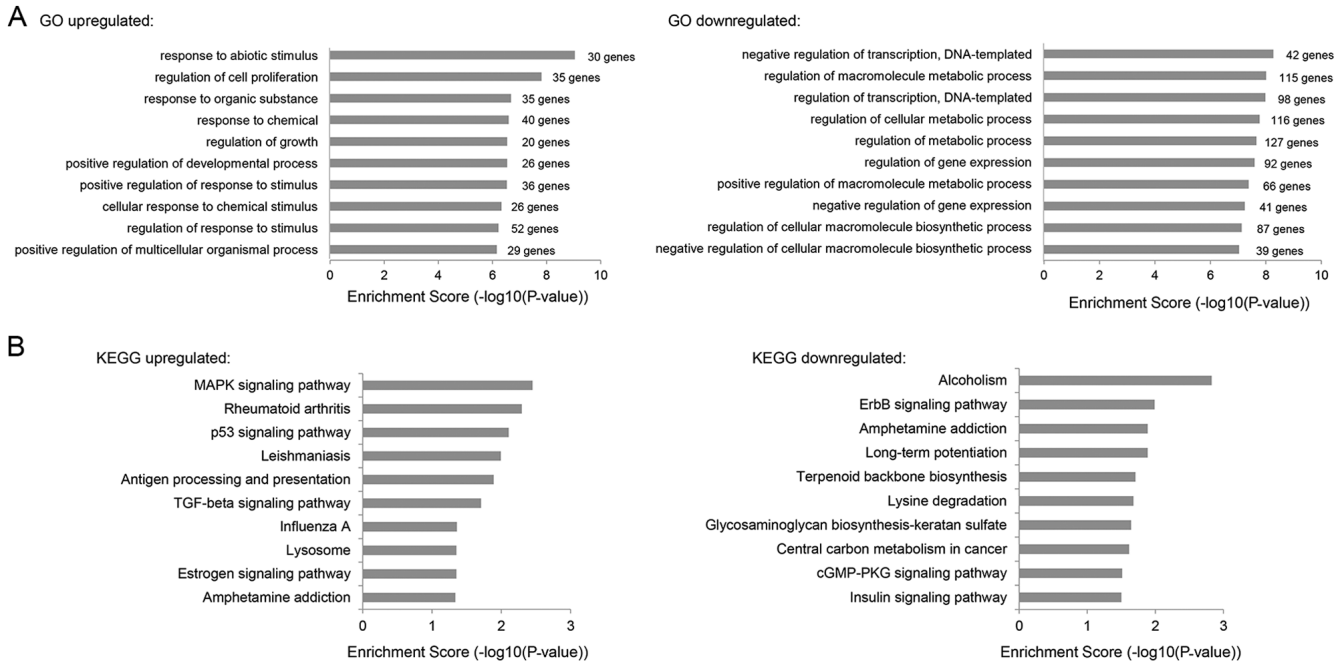

Figure 5. GO and KEGG analyses of RNA-seq data. (A) Analysis of GO term enrichment of the biological process category of genes with increased (left) or decreased (right) expression after SUV420H2 depletion. The top 10 GO terms based on the P-value are plotted. (B) KEGG pathway enrichment analysis of up (left) or downregulated (right) genes identified in SUV420H2 deleted HOS cells. cGMP-PKG, cyclic GMP-dependent protein kinase; ErbB2, erb-b2 receptor protein kinase 2; GO, Gene Ontology; KEGG, Kyoto Encyclopedia of Genes and Genomes; MAPK, mitogen-activated protein kinase; SUV420H2, lysine methyltransferase 5C; TGF, transforming growth factor.

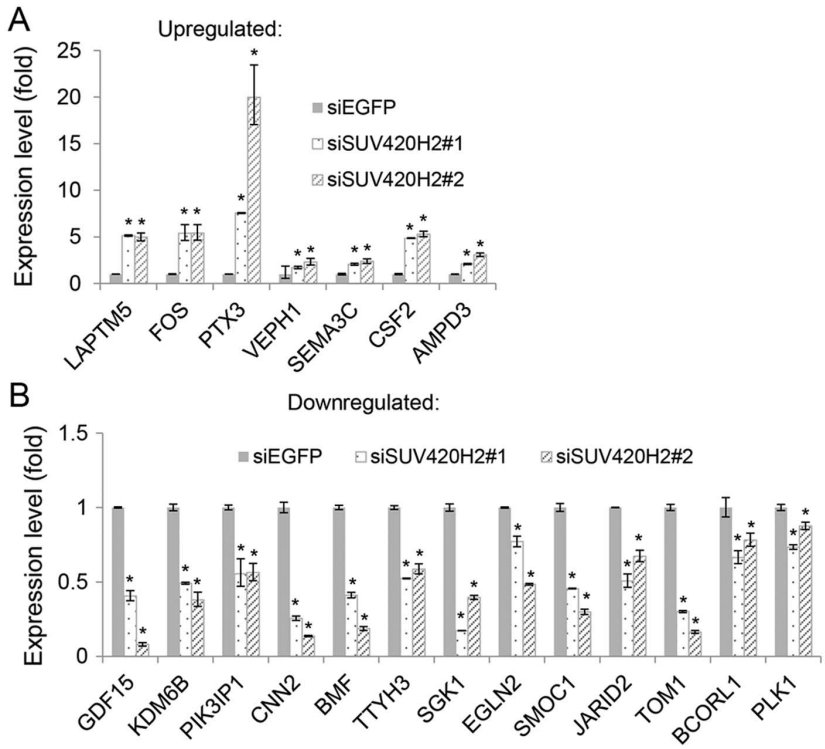

Figure 6. Validation of RNA-sequencing results using RT-qPCR. Expression of selected SUV420H2-associated genes, including (A) upregulated and (B) downregulated genes upon SUV420H2 depletion, was validated in control (siEGFP) and SUV420H2-depleted (siSUV420H2#1 and siSUV420H2#2) HOS cells using RT-qPCR analysis. The relative mRNA expression levels (normalized to GAPDH) in siSUV420H2#1 and siSUV420H2#2 samples were compared to that in the control siEGFP sample. Data are presented as the mean ± SEM of three experimental repeats; $^{*}P<0.05$, siSUV420H2 vs. siEGFP. RT-qPCR, reverse transcription-quantitative PCR; si, small interfering RNA; LAPTM5, lysosomal protein transmembrane 5; FOS, Fos proto-oncogene; PTX3, pentraxin 3; VEPH1, ventricular zone expressed PH domain containing 1; SEMA3C, semaphorin 3C; CSF2, colony stimulating factor 2; AMPD3, adenosine monophosphate deaminase 3; GDF15, growth differentiation factor 15; KDM6B, lysine demethylase 6B; PIK3IP1, phosphoinositide-3-kinase interacting protein 1; CNN2, calponin 2; BMF, Bcl2 modifying factor; TTYH3, tweety family member 3; SGK1, serum/glucocorticoid regulated kinase 1; EGLN2, egl-9 family hypoxia inducible factor 2; SMOC1, SPARC related modular calcium binding 1; JARID2, jumonji and AT-rich interaction domain containing 2; TOM1, target of myb1 membrane trafficking protein; BCORL1, BCL6 corepressor like 1; PLK1, polo-like kinase 1.

of H4K20me3 in OS tissue samples and cancer cell lines. The results found decreased levels of H4K20me3 in OS tissue samples and cell lines compared with normal samples. These findings indicated that the loss of H4K20me3 is likely to be involved in the development and progression of OS.

SUV420H proteins, including SUV420H1 and SUV420H2, mediate the vast majority of H4K20me3 modifications (33). In SUV420H1-null primary mouse embryonic fibroblasts, H4K20me2, but not H4K20me3, is reduced. In contrast, SUV420H2-null cells exhibit selective loss of H4K20me3, but maintain H4K20me2, indicating that SUV420H2 has a preference to induce H4K20me3 (23). In order to further elucidate which histone methyltransferase are responsible for the loss of H4K20me3 in OS, the expression levels of SUV420H1 and SUV420H2 were investigated in OS cell lines. Notably, there was a pronounced decrease in SUV420H2 expression levels in OS cells, whereas no significant changes were detected in the expression levels of SUV420H1. These findings suggested that aberrant SUV420H2 expression was largely associated with the loss of H4K20me3 in OS cells. However, the protein expression levels of SUV420H1 were unable to be examined in the present study due to specificity issues with the available antibodies. Similarly, reduced expression levels of SUV420H2 are also observed in breast cancer, lung cancer, liver cancer and colon cancer (12,13,34). In addition, the expression of SUV420H2 was found to have no prognostic value for patients with OS; however, this may be due to the limited small sample size in the present study. Despite a lack of significance being observed in the present study, there was some tendency for SUV420H2 expression to be associated with a poorer prognosis, implying that SUV420H2 and H4K20me3 may have value as prognostic factors in OS. To clarify this, the expression levels of SUV420H2 and H4K20me3 in OS tissue samples should be examined with a larger sample size. Unfortunately, due to issues with antibody-specificity for targeting SUV420H2, the present study was unable to examine the expression levels of SUV420H2 in OS tissue samples.

Transient depletion of SUV420H2 results in a decreased expression of several osteoblastic markers, such as integrin binding sialoprotein and alkaline phosphatase, biomineralization associated, as well as osteoblastic transcription factors, such as Sp7 transcription factor (35). To the best of our knowledge, there is limited information regarding the functions of SUV420H2 as well as H4K20me3 in OS. To explore the involvement of SUV420H2 in the development and progression of OS, SUV420H2 regulated genes were identified through RNA-seq analysis. GO term enrichment analysis using SUV420H2 regulated genes revealed that as well as regulation of cell proliferation, transcription and gene expression, SUV420H2 was also likely to be involved in the response to abiotic stimulus (GO:0009628), cellular response to chemical stimulus (GO:0070887), regulation of response to stimulus (GO:0048583), and metabolic processes (GO:0019222, regulation of metabolic process; GO:0031323, regulation of cellular metabolic process; GO:0080090, regulation of primary metabolic process). Furthermore, SUV420H2 expression was found to be associated with MAPK, P53, TGF and ErbB signaling pathway through regulations of the lysosomal protein transmembrane 5, *FOS* and phosphoinositide-3-kinase interacting protein 1 genes. Further studies should focus on confirming that there has been accumulation of H4K20me3 within these targeted genes in SUV420H2-overexpressing OS cells.

In conclusion, the present study revealed that aberrations in SUV420H2 expression and the resultant loss of H4K20me3 in OS may be important factors for further understanding the biological significance of SUV420H2 and H4K20me3 in OS. However, further studies are required to elucidate the underlying mechanisms of action behind the involvement of SUV420H2 and H4K20me3 in OS through the regulation of the aforementioned genes.

Acknowledgements

The authors would like to thank Professor Shan Chang (Institute of Bioinformatics and Medical Engineering, Jiangsu University of Technology) for their support.

Funding

The present study was supported by The National Natural Science Foundation of China (grant no. 81903661) and Changzhou Sci&Tech Program (grant no. 20180170).

Availability of data and materials

The datasets used and/or analyzed in the present study are available from the corresponding author on reasonable request.

Authors' contribution

LP and XY participated in the whole project and performed the majority of the experiments. LW, XX and MZ performed immunohistochemistry-related experiments. JL and RK analyzed RNA-seq data. ZL was involved in the conception of the study and also supervised the quality of all the work throughout the entire process. All authors read and approved the final manuscript.

Ethics approval and consent to participate

Not applicable.

Patient consent for publication

Not applicable.

Competing interests

The authors declare that there is no competing interest associated with the manuscript.

References

1. Morrow JJ and Khanna C: Osteosarcoma genetics and epigenetics: Emerging biology and candidate therapies. Crit Rev Oncog 20: 173-197, 2015.
2. Hattinger CM, Fanelli M, Tavanti E, Vella S, Ferrari S, Picci P and Serra M: Advances in emerging drugs for osteosarcoma. Expert Opin Emerg Drugs 20: 495-514, 2015.
3. Martin JW, Squire JA and Zielenska M: The genetics of osteosarcoma. Sarcoma 2012: 627254, 2012.
4. Luco RF, Pan Q, Tominaga K, Blencowe BJ, Pereira-Smith OM and Misteli T: Regulation of alternative splicing by histone modifications. Science 327: 996-1000, 2010.
5. Huertas D, Sendra R and Muñoz P: Chromatin dynamics coupled to DNA repair. Epigenetics 4: 31-42, 2009.

6. Greer EL and Shi Y: Histone methylation: A dynamic mark in health, disease and inheritance. Nat Rev Genet 13: 343-357, 2012.
7. Hamamoto R, Saloura V and Nakamura Y: Critical roles of non-histone protein lysine methylation in human tumorigenesis. Nat Rev Cancer 15: 110-124, 2015.
8. Balakrishnan L and Milavetz B: Decoding the histone H4 lysine 20 methylation mark. Crit Rev Biochem Mol Biol 45: 440-452, 2010.
9. Jorgensen S, Schotta G and Sorensen CS: Histone H4 lysine 20 methylation: Key player in epigenetic regulation of genomic integrity. Nucleic Acids Res 41: 2797-2806, 2013.
10. Kwon MJ, Kim SS, Choi YL, Jung HS, Balch C, Kim SH, Song YS, Marquez VE, Nephew KP and Shin YK: Derepression of CLDN3 and CLDN4 during ovarian tumorigenesis is associated with loss of repressive histone modifications. Carcinogenesis 31: 974-983, 2010.
11. Fraga MF, Ballestar E, Villar-Garea A, Boix-Chornet M, Espada J, Schotta G, Bonaldi T, Haydon C, Ropero S, Petrie K, *et al*: Loss of acetylation at Lys16 and trimethylation at Lys20 of histone H4 is a common hallmark of human cancer. Nat Genet 37: 391-400, 2005.
12. Pogribny IP, Ross SA, Tryndyak VP, Pogribna M, Poirier LA and Karpinets TV: Histone H3 lysine 9 and H4 lysine 20 trimethylation and the expression of Suv4-20h2 and Suv-39h1 histone methyltransferases in hepatocarcinogenesis induced by methyl deficiency in rats. Carcinogenesis 27: 1180-1186, 2006.
13. Tryndyak VP, Kovalchuk O and Pogribny IP: Loss of DNA methylation and histone H4 lysine 20 trimethylation in human breast cancer cells is associated with aberrant expression of DNA methyltransferase 1, Suv4-20h2 histone methyltransferase and methyl-binding proteins. Cancer Biol Ther 5: 65-70, 2006.
14. Van Den Broeck A, Brambilla E, Moro-Sibilot D, Lantuejoul S, Brambilla C, Eymin B and Gazzeri S: Loss of histone H4K20 trimethylation occurs in preneoplasia and influences prognosis of non-small cell lung cancer. Clin Cancer Res 14: 7237-7245, 2008.
15. Schneider AC, Heukamp LC, Rogenhofer S, Fechner G, Bastian PJ, von Ruecker A, Müller SC and Ellinger J: Global histone H4K20 trimethylation predicts cancer-specific survival in patients with muscle-invasive bladder cancer. BJU Int 108: E290-E296, 2011.
16. Benard A, Goossens-Beumer IJ, van Hoesel AQ, de Graaf W, Horati H, Putter H, Zeestraten EC, van de Velde CJ and Kuppen PJ: Histone trimethylation at H3K4, H3K9 and H4K20 correlates with patient survival and tumor recurrence in early-stage colon cancer. BMC Cancer 14: 531, 2014.
17. Yokoyama Y, Matsumoto A, Hieda M, Shinchi Y, Ogihara E, Hamada M, Nishioka Y, Kimura H, Yoshidome K, Tsujimoto M and Matsuura N: Loss of histone H4K20 trimethylation predicts poor prognosis in breast cancer and is associated with invasive activity. Breast Cancer Res 16: R66, 2014.
18. Paydar P, Asadikaram G, Nejad HZ, Akbari H, Abolhassani M, Moazed V, Nematollahi MH, Ebrahimi G and Fallah H: Epigenetic modulation of BRCA-1 and MGMT genes, and histones H4 and H3 are associated with breast tumors. J Cell Biochem 120: 13726-13736, 2019.
19. Wu Y, Shi W, Tang T, Wang Y, Yin X, Chen Y, Zhang Y, Xing Y, Shen Y, Xia T, *et al*: miR-29a contributes to breast cancer cells epithelial-mesenchymal transition, migration, and invasion via down-regulating histone H4K20 trimethylation through directly targeting SUV420H2. Cell Death Dis 10: 176, 2019.
20. Özgür E, Keskin M, Yörüker EE, Holdenrieder S and Gezer U: Plasma histone H4 and H4K20 trimethylation levels differ between colon cancer and precancerous polyps. In vivo 33: 1653-1658, 2019.
21. Yang H, Pesavento JJ, Starnes TW, Cryderman DE, Wallrath LL, Kelleher NL and Mizzen CA: Preferential dimethylation of histone H4 lysine 20 by Suv4-20. J Biol Chem 283: 12085-12092, 2008.
22. Sakaguchi A, Karachentsev D, Seth-Pasricha M, Druzhinina M and Steward R: Functional characterization of the Drosophila Hmt4-20/Suv4-20 histone methyltransferase. Genetics 179: 317-322, 2008.
23. Schotta G, Sengupta R, Kubicek S, Malin S, Kauer M, Callén E, Celeste A, Pagani M, Opravil S, De La Rosa-Velazquez IA, *et al*: A chromatin-wide transition to H4K20 monomethylation impairs genome integrity and programmed DNA rearrangements in the mouse. Genes Dev 22: 2048-2061, 2008.
24. Benetti R, Gonzalo S, Jaco I, Schotta G, Klatt P, Jenuwein T and Blasco MA: Suv4-20h deficiency results in telomere elongation and derepression of telomere recombination. J Cell Biol 178: 925-936, 2007.
25. Marion RM, Schotta G, Ortega S and Blasco MA: Suv4-20h abrogation enhances telomere elongation during reprogramming and confers a higher tumorigenic potential to iPS cells. PLoS One 6: e25680, 2011.
26. Livak KJ and Schmittgen TD: Analysis of relative gene expression data using real-time quantitative PCR and the 2(-Delta Delta C(T)) method. Methods 25: 402-408, 2001.
27. Trapnell C, Roberts A, Goff L, Pertea G, Kim D, Kelley DR, Pimentel H, Salzberg SL, Rinn JL and Pachter L: Differential gene and transcript expression analysis of RNA-seq experiments with TopHat and Cufflinks. Nat Protoc 7: 562-578, 2012.
28. Tian L, Greenberg SA, Kong SW, Altschuler J, Kohane IS and Park PJ: Discovering statistically significant pathways in expression profiling studies. Proc Natl Acad Sci USA 102: 13544-13549, 2005.
29. Eferl R and Wagner EF: AP-1: A double-edged sword in tumorigenesis. Nat Rev Cancer 3: 859-868, 2003.
30. Strelau J, Bottner M, Lingor P, Suter-Crazzolara C, Galter D, Jaszai J, Sullivan A, Schober A, Krieglstein K and Unsicker K: GDF-15/MIC-1 a novel member of the TGF-beta superfamily. Journal of neural transmission. J Neural Transm Suppl: 273-276, 2000.
31. Strahl BD and Allis CD: The language of covalent histone modifications. Nature 403: 41-45, 2000.
32. Kouzarides T: Chromatin modifications and their function. Cell 128: 693-705, 2007.
33. Schotta G, Lachner M, Sarma K, Ebert A, Sengupta R, Reuter G, Reinberg D and Jenuwein T: A silencing pathway to induce H3-K9 and H4-K20 trimethylation at constitutive heterochromatin. Genes Dev 18: 1251-1262, 2004.
34. Shinchi Y, Hieda M, Nishioka Y, Matsumoto A, Yokoyama Y, Kimura H, Matsuura S and Matsuura N: SUV420H2 suppresses breast cancer cell invasion through down regulation of the SH2 domain-containing focal adhesion protein tensin-3. Exp Cell Res 334: 90-99, 2015.
35. Khani F, Thaler R, Paradise CR, Deyle DR, Kruijthof-de Julio M, Galindo M, Gordon JA, Stein GS, Dudakovic A and van Wijnen AJ: Histone H4 methyltransferase Suv420h2 maintains fidelity of osteoblast differentiation. J Cell Biochem 118: 1262-1272, 2017.